Physiological characterization and gene mapping of a novel cuticular wax-related mutant in barley

Yunxia Fang
Hangzhou Normal University
Xiaoqin Zhang
Hangzhou Normal University
Tao Tong
Hangzhou Normal University
Ziling Zhang
Hangzhou Normal University
Bin Tian
Hangzhou Normal University
Jun Cui
Hangzhou Normal University
Junjun Zheng
Hangzhou Normal University
Dawei Xue (dwxue@hznu.edu.cn)
Hangzhou Normal University https://orcid.org/0000-0001-9904-7615

Research article

Keywords: Cuticular waxes, Crystal shapes, Genetic mapping, SLAF-seq, Barley

Posted Date: February 5th, 2020

DOI: https://doi.org/10.21203/rs.2.22665/v1

Abstract

Background: Cuticular wax is a type of lipid covering the surface of plants, which is directly related to crop stress resistance. Thus, it is important to study wax-related genes and their regulatory mechanism in wax biosynthesis pathway for improving stress resistance.

Results: In this study, a wax-deficient barley mutant *barley cuticular wax1*（*bcw1*）was identified, and genetic analysis indicated that the trait was controlled by a single recessive nuclear gene. Phenotype observations showed that the tubule-shaped waxy crystals covering the sheath and stem epidermis of mutants disappeared, but there was no significant differences were detected in the leaf epidermis between mutant and wild type. Water loss data confirmed that the cuticular waxes and cutins improved plant resistance to drought stress. By combining the bulk segregant analysis (BSA) and specific locus amplified fragment sequencing (SLAF-seq) strategy, the wax-related gene *BCW1* was located on chromosome 2 with a total length of 15.10 Mb. No cuticular wax-related genes have been reported in the regions, indicating that *BCW1* is a novel gene that plays roles in cuticular wax biosynthesis and wax crystals formation.

Conclusions: The research showed that mutation of *BCW1* did not affect the crystal shape or cutin formation outside the leaf surfaces, but decreased the wax and cutin accumulation outside stems and sheaths. Therefore, our work provides the basis for the cloning of *BCW1* and studying of the crystal self-assembly mechanism.

Background

Cuticular waxes, primarily composed of very long chain fatty acids(C20-C34) and their derivatives, cover the surface of most organs in the shoots of terrestrial plants [1, 2]. Together with the reticular structure cuticle outside the epidermal cells, cuticular waxes form a hydrophobic barrier for plant self-protection [3–5]. As a natural protective layer for plants, cuticular waxes play an important role in the plant response to external biotic and abiotic stresses, such as water loss prevention, high temperature resistance, protection against pathogen invasion and plant-eating insects [5–7].

It is important to study the metabolic process of cuticular wax and its related regulatory genes for improving plant stress resistance. Currently, a large number of wax-related genes involved in stress resistance have been isolated and cloned in many plants [4, 7–9]. Although several wax-related mutants have been identified in barley (Hordeum vulgare L.), some have been localized and only a few have been cloned. In total, 27 eceriferum (cer) loci that have been linked to the Barley BinMap 2005(https://wheat.pw.usda.gov/cgi-bin/GG3/report.cgi?class=mapdata). Among them, mutant cer-zv was positioned in a pericentromeric region on chromosome 4, and co-separated with marker AK251484 [10]. The cer-zg locus was also located on 4H and completely linked to wax-synthesis gene HvCER6, which may be the candidate gene for cer-zg [11]. Both cer-zv and cer-zg were sensitive to drought, and lost water quickly under drought stress. The Cer-b.2, a mutant gene involved in β-diketone metabolism,

was located on 3HL between gene markers MLOC_10972 and MLOC_69561 [12]. EIBI1, the first waxy-related gene cloned from wild barley, encodes a full transporter of ABC transporter G subfamily that is responsible for transporting keratinocyte from cells to the leaf surface to form cuticle [13]. Loss of function mutants, such as cer-zh and cer-zv, exhibit thinner cutins on the leaf surface, and result in rapid water loss, poor water retention and lower drought resistance [10, 13, 14]. Both HvKCS6 and CER-ZH/HvKCS1 encode ketoacyl-CoA synthase (KCS), which is involved in wax synthesis, and whose mutation decreases the cuticle water-barrier properties and resistance to powdery mildew fungi of mutants [6, 14]. The Cer-c, -q and-u mutant genes were located in the subtelomere region of 2HS and formed a gene cluster (Cer-cqu). Sequence analysis revealed that the mutants encode β-diketone synthase (DKS), lipase/carboxyl transferase and P450, respectively, and participated in the synthesis of plant cuticular wax [15, 16].

Due to the large amount of genomic data and numerous repetitive sequences [17], it is difficult to develop polymorphic markers among barley varieties. Specific locus amplified fragment sequencing (SLAF-seq) is a simplified genome sequencing technology based on high-throughput sequencing, that reduces the complexity of the genome through enzymatic digestion[18]. A large number of SLAF tags can be obtained from SLAF-sEq. Subsequently, genotyping and molecular marker development, especially single nucleotide polymorphism (SNP) markers, are conducted according to the polymorphic analysis among SLAF tags [18, 19]. SLAF-seq technology used for developing SNP markers is an excellent strategy for rapidly obtaining abundant specific sites and has been applied for genetic map construction and QTL analysis [19–21]. Bulked segregant snalysis (BSA) is a rapid method used for locating target genes or major QTLs that control target traits by constructing "gene pools" [22]. The combination of SLAF-seq and BSA has been proved to be effective for identifying major QTLs or candidate gene. This combination has been successfully used in rice [23], cucumber [24], barley [25, 26], wheat [27], tomato [28], and pepper [29].

In this study, a barley cuticular wax mutant barley cuticular wax 1 (bcw1) was identified from an ethyl methanesulfonate (EMS) mutagenesis population. Compared with the wild type, no significant differences were detected between leaves. However, litter cuticular waxes were found on the surface of stems and sheaths, and the total wax content reduced significantly. Genetic analysis revealed that the trait was controlled by a recessive gene. Based on SLAF-BSA technology, a total of 48,110 high-quality SNPs were obtained and analyzed. The results showed that the wax-deficient gene BCW1 was initially located within 9 intervals of 15.10 Mb on chromosome 2. This work provides a basis for the fine mapping and cloning of BCW1, and identifies an ideal mutant for investigating the self-assembly molecular mechanism of wax crystals.

Results

The bcw1 mutant displayed glossy stems and sheaths.

The cuticular waxes of bcw1 and wild type ZJU3 were observed throughout the whole growth period. No significant differences were detected at seedling stage (Additional file 1: Figure S1), but the mutant

phenotype would be gradually appeared after tilling stage. Comparing the phenotype characteristics between the ZJU3 and bcw1, the results showed that the stems and sheaths of wild type were covered with a layer of white powder, which made the stem and leaf sheath surface glaucous, while the stem and sheath surface of mutant were glossy (Fig. 1a-c). In addition, epicuticular wax crystals of the plants are spherical droplets, which prevent water from staying on the surface of plant epidermis and avert the deposition of dust, pollutants and pathogen spores [32]. Therefore, water was sprayed onto the surface of bcw1 and ZJU3, A series of water droplets that formed and attached on the stem and sheath surface of mutants were observed, but no water droplets or water residue formed on the surface of ZJU3 (Fig. 1d, e), which confirmed that the cuticular waxes were defective in bcw1.

Genetic analysis of wax-deficient mutant bcw1

To analysis the inheritance behavior of bcw1, a genetic analysis was conducted on F1 plants and F2 populations, which developed from the crosses between bcw1 and Morex, and bcw1 and X188. All F1 hybrid plants exhibited glaucous surfaces and all glaucous and glossy plants in F2 segregating population were counted, respectively (Table 1). The χ^2 test results showed that the genetic separation ratio of the two populations was in accordance with the Mendelian segregation of 3:1($\chi^2 < \chi^2_{0.05,1} = 3.84$), indicating that the mutant trait was controlled by a single recessive nuclear locus.

Table 1
Statistical analysis of genetic populations

Crosses	F_1 plants	F_2 populations				
		Glaucous plants	Glossy plants	Total plants	$\chi^2_{3:1}$	$\chi^2_{0.05}$
bcw1 × Morex	Glaucous	157	50	207	0.23	3.84
bcw1 × X188	Glaucous	179	56	235	0.28	3.84

Defective wax crystals on stem and sheath surfaces of bcw1

To confirm whether epicuticular wax crystals of bcw1 were affected, SEM observations were conducted on the stem, sheath and leaf epidermis of wild type and mutant plants. Results revealed that the epicuticular wax structures covering the stem and sheath surfaces of the bcw1 were different from the wild type (Fig. 2). The stem and sheath surfaces of ZJU3 were covered with a dense waxy layer, which exhibited tubule-shaped, overlapping and interlacing (Fig. 2a, b), but only little wax crystals were deposited on bcw1 tissue surface (Fig. 2d, e). However, there were no obvious differences detected in the platelet-shaped waxy crystals distributed on the leaf surface between bcw1 and ZJU3 (Fig. 2c, f).

Altered cuticles of stems and sheaths in bcw1

The reticular cutin is filled with cuticular wax and forms a dense cuticle that protects plants from external stress [4]. During this process, abnormal deposition of cuticular wax may cause aberrant cuticle formations in some tissues. Therefore, TEM observations were conducted on stem, sheath and leaf cuticles of bcw1 and wild type. Similar to the SEM observation results, cuticles outside the epidermal cells of bcw1 stems and leaf sheaths were thinner, looser and irregular compared to the wild type (Fig. 3a, b, d, e), while the leaf cuticles of bcw1 were normal (Fig. 3c, f).

Decreased total cuticular waxes of bcw1 stem and sheath surfaces.

Based on the SEM and TEM observations and due to the abnormal epicuticular wax structures and cuticles of bcw1, the total wax contents were measured. The result indicated that the total wax contents of bcw1 stems and leaf sheaths were significantly lower than ZJU3 (Fig. 4), Although the epicuticular waxes from leaves of bcw1 were slightly changed, there was no significant difference were detected compared to ZJU3, which was consistent with the results of SEM and TEM observation.

Altered water loss rate of detached stems and sheaths.

In order to evaluate the drought resistance of bcw1, water loss rate was measured. Results showed that the values of detached sheaths and stems of bcw1 were higher than ZJU3 in vitro (Fig. 5b, c). Moreover, the water loss rate of bcw1 sheaths and stems increased extremely compared to ZJU3 after 3.5 hours in vitro time, and the difference became increasingly significant at subsequent in vitro time (Fig. 5). In addition, although the water loss rate of detached leaves of bcw1 were slightly higher than ZJU3, no significant differences were detected at any time points (Fig. 5a).These results were in agreement with the distribution of epidermis waxes of bcw1 and ZJU3, which indicated that the absence of bcw1 epidermis wax resulted in faster in vivo water loss, reducing water-holding capacity and increasing sensitivity to drought.

SLAF tag development and high-quality SNP screening

According to the SLAF library construction and high-throughput sequencing, a total of 154,410,911 valid reads were obtained, of which the guanine-cytosine (GC) content comprised 44.57%, and the Q30 value was more than 90%. In addition, the similarity between samples and reference genomes was above 97%, indicating that the samples were not contaminated and could be subsequently compared and detected (Additional file 2: Table S1). Moreover, 327,186 SLAF tags were developed and mapped to the whole assembly genome of barley (Additional file 3: Table S2; Additional file 4: Figure S2). Based on the SLAF - tags in four samples, 1,290,839 SNPs were developed. In order to ensure the accuracy, SNPs that did not conform to population genetic characteristics and whose reads were less than 4 were exluded. A total of 48,110 high-quality SNP markers were obtained (Additional file 5: Table S3).

Association regions of wax-related gene in barley

All high-quality SNP markers were used for association analysis, and the results showed that intervals calculated by the SNP-index algorithm were located on chromosome 2 (Additional file 6: Figure S3).

According to the theoretical segregation ratio of the F2 population and the ΔSNP-index threshold value, 9 discontinuous regions between 431,198,045 bp and 509,725,587 bp were obtained, which may be candidate regions of the wax-related gene BCW1. The total length of the 9 intervals was 15.10 Mb and 301 genes were predicted in the region (Table 2). By comparing the physical location of Cer-cqu gene cluster previously reported on chromosome 2 [15, 16], BCW1 was found to be a novel wax-related gene in barley.

Table 2
Association regions detected using the ΔSNP-index method

Association analysis	Chr.	Start	End	Size(Mb)	Gene Number
ΔSNP-index	2H	431,198,045	431,399,953	0.20	2
	2H	432,644,702	434,325,458	1.68	26
	2H	481,972,512	493,301,085	11.33	206
	2H	493,926,763	493,964,804	0.04	6
	2H	501,875,587	501,949,702	0.07	1
	2H	502,990,223	503,071,606	0.08	2
	2H	505,971,530	506,326,788	0.36	6
	2H	506,565,656	507,427,086	0.86	37
	2H	509,245,316	509,725,587	0.48	15

Discussion

Epidermal wax synthesis, transportation and regulation is a complex biological process that plays an important role in stress resistance, in which lots of regulatory factors and gene families are involved [2, 3]. In this study, a wax-deficient mutant bcw1 in barley was identified and exhibited glossy leaf sheaths and stems phenotypes (Fig. 1b, c). Interestingly, there were no obvious phenotypic differences between leaf surfaces of ZJU3 and bcw1, but a white powder layer distributing on stem and sheath surfaces were defective in bcw1(Fig. 1a-c). Moreover, the total cuticular wax content of stems and sheaths was decreased significantly in bcw1, and the leaves exhibited no differences between wild-type and bcw1, indicating that the cuticular waxes were absent on the stem and sheath surfaces of bcw1 (Fig. 4). Moreover, the water drops results also confirmed these conclusions (Fig. 1d, e).

The tubule-shaped and platelet-shaped crystals are resulted from the accumulations of cuticular waxes, which were regulated by different molecular self-assembly process [33–35]. Previous studies demonstrated that the main component of tubule-shaped crystals is β-diketone, while the main component of platelet -shaped crystals is primary alcohols [33–35]. Mutants with altered waxy crystal structures have been identified in barley, but exhibited different characteristics [10, 12, 14, 36, 37]. Among

them, the cer-b.2 exhibited non-glaucous leaf sheaths, on which epicuticular waxes formed platelet-shaped crystals rather than tubule-shaped crystals, due to β-diketone deficiency that was compensated by primary alcohols [12]. The altered crystals shape was also observed in the cer-cqu barley mutant, which was defective in the β-diketone biosynthesis pathway [15, 16]. The cer-zh displayed glossy leaf blades due to the large decrease in primary alcohols [14]. Based on the SEM observations in this study, tubule-shaped waxy crystals depositing on the stem and leaf sheath surfaces were absent in bcw1 (Fig. 2), but platelet-shaped waxy crystals distributing on the leaf surfaces were almost the same as wild-type (Fig. 2c, f). Therefore, the wax crystal structures of bcw1 were different from other previously identified mutants, indicating that it may be controlled by different genetic mechanisms.

Although both cutins and epicuticular waxes are located outside the epidermis cells, the cutins form earlier than cuticular wax deposition and the chemical compositions are different [38–40]. In fact, cuticular wax deficiency also affects the cutin depositions. For example, the Cer-zh mutation decreased the wax synthesis of leaf surfaces, and changed cutin composition [14]. Water loss rate is an important physiological index for evaluating the drought resistance of plants, and epicuticular waxes play critical roles in decreasing non-stomatal water loss under drought condition [1, 5, 10]. Moreover, the mount of cutins also affects water loss [40]. For instance, barley mutants with thinner cutin were more sensitive to drought, such as cer-zv and eibi1 [10, 13, 37]. In this study, the detached leaf sheaths and stems of bcw1 lost water more rapidly than wild type at room temperature (Fig. 5). Except for epicuticular wax deficiency, the sheaths and stems of bcw1 also showed much thinner cutins than ZJU3 (Fig. 2, 3), suggesting that the two factors increased the non-stomatal water loss in bcw1.

SLAF-seq is an efficient strategy for developing a large number of high-accuracy SNP markers, which can be used for genotyping and constructing high-density genetic linkage maps [19–21, 41]. Additionally, the combination of SLAF-seq and BSA analysis is a fast and cost-effective method for locating functional genes [23, 24, 42]. In this study, genetic analysis suggested that the wax-deficient phenotype of bcw1 was controlled by a single recessive locus (Table 1). Therefore, two pools of mutant and wild-type plants were selected from the F2 population and prepared for SLAF-seq analysis. Then, SLAF-tags were obtained based on the analysis of reads, and large-scale SNP markers were screened (Additional file 3: Table S2; Additional file 5: Table S3). Association analysis was conducted using the SNP-index algorithm. As a result, BCW1 was mapped to 9 intervals on chromosome 2 (Additional file 4: Figure S2; Table 2). No wax-related genes were reported in these regions; therefore, BCW1 can be considered an unreported novel gene. However, the 9 intervals were as long as 15.10 Mb, which was larger than the candidate region of 0.19 MB and 0.24 MB in cucumber and rice, respectively [23, 24]. Similarly, the black lemma and pericarp gene in barley is also initial mapped to a region of 32.41 MB using the SLAF-BSA method [26], which could be attributed to the genomes size and sequence structure. The barley genome is ~ 5.3 Gb and contains many repeat sequences [17]. When SLAF-seq technology is used by enzyme cutting and sequencing, it affects the uniform distribution of enzyme cutting sites in the genome, which may subsequently affect the accuracy of localization.

Conclusions

The wax-deficient mutant, bcw1 was identified and mapped on chromosome 2H in this study. There have been no wax-related genes were reported in these regions, indicating that BCW1 is a novel gene. Mutation of BCW1 did not affect the crystal shape or cutin formation outside the leaf surfaces, but decreased the wax and cutin accumulation outside stems and sheaths. The deposition processes of both were unclear, thus bcw1 is considered a candidate gene for the study of self-assembly molecular mechanism. Additionally, high quality-SNP markers were obtained in the candidate regions, which will be beneficial for the fine mapping and cloning of BCW1 in future studies.

Methods

Plant materials

The cuticular wax-deficient mutant bcw1 was obtained by EMS mutagenesis of Zhenongda 3 (ZJU3) [43] and was crossed with two normal barley varieties, Morex and X188, to construct F1 and F2 populations. The phenotypes of the F1 and F2 progenies were observed at heading stage, and the number of normal and mutant phenotypic plants in two F2 segregated populations was recorded. All the experimental materials were planted in Hangzhou, Zhejiang Province.

Cuticular wax observation by SEM and TEM

At grain filling stage, the leaves, stems and sheaths of bcw1 and ZJU3 were cut and fixed in 2.5% glutaraldehyde solution for 4 hours. Then, samples were washed with PBS solutionand fixed again in 1% osmium acid solution for 2 hours at 4℃. Fixed samples were dehydrated in a graded series of ethanol, dried with CO_2 in a critical point dryer, and coated with gold under vacuum. The prepared specimens were observed using a SU-8010 scanning electron microscope (SEM, Hitachi). Additionally, parts of the fixed samples were dehydrated with graded acetone and soaked in acetone-resin mixtures and pure resin, respectively. Finally, samples were embedded in resin. Ultrathin sections collected and observed by Tecnai G2 Spirit transmission electron microscopy (TEM, FEI Co.).

Extraction of the total cuticular waxes

Leaves, stems and sheaths of ZJU3 and bcw1 at heading stage were sampled, and fresh weight of the samples was weighed, respectively. Then, samples were immersed in 30 mL chloroform for 2 minutes, and the total cuticular waxes were extracted into chloroform. Each sample was repeated three times. The extract was transferred into an empty beaker with known weight and placed in a ventilation system for drying. Sample beakers and empty beakers were weighed by a microbalance (d = 0.0001). The deposition of wax was expressed by the waxy content per unit fresh weight of epidermis wax (mg.g-1 FW).

Determination of water loss rate

The water loss rate was determined by the natural drying method. Leaves, sheaths and stems of bcw1 and ZJU3 at flowering stage were sampled and dried naturally at room temperature. At seven time points,

all detached samples were weighed to calculate the water loss rate. The experiment was repeated five times. Water loss was calculated as follows:

Water loss rate = ((W1-W2)/W1) × 100%

Where W1 is the initial weight of the leaves, sheaths or stems; W2 is the weight of leaves, sheaths or stems measured at seven time points.

Construction of DNA pools

The F2 segregated population generated by crossing the mutant with X188 was selected for SLAF-seq analysis. According to BSA method, 30 plants with mutant phenotype and normal cuticular waxes were randomly selected from F2 population, respectively, to construct mutant pool and wild type pool. Meanwhile, ZJU3 and homozygous mutant DNA were also extracted for subsequent experimental analysis.

Large-scale SNP markers development and screening

Based on the SLAF-seq method [18, 19], DNA fragments were isolated and tested for high-quality SLAF library construction and high-throughput sequencing. The obtained reads were compared to the barley reference genome (ftp://ftp.ensemblgenomes.org/pub/plants/release-34/fasta/hordeum_vulgare/dna/), then SNP markers were developed and analyzed. Based on the differences between allele numbers and genotype sequences of four DNA pools, high-quality SNP markers were screened for the initial mapping of BCW1.

Association analysis of the wax-related gene BCW1

The SNP-index algorithm, which is mainly used for determing significant differences in genotype frequencies between mixed DNA pools, was used to perform association analysis [30, 31]. SNPs identified between the pools were regarded as polymorphic for the association studies. The ΔSNP-index indicates the difference in genotype frequencies, and the closer this value is to theoretical threshold, the stronger association between SNPs and a given trait.

Abbreviations

SLAF-seq: specific locus amplified fragment sequencing; BSA: bulk segregant analysis; SNPs: single nucleotide polymorphism markers

Additional Files

Additional files

Additional file 1: Figure S1 The leaf phenotype of bcw1 and ZJU3 at seedling stage

Additional file 2: Table S1 Statistics of the sequencing data for each sample

Additional file 3: Table S2 Distribution of SLAF tags and SNPs on each chromosome

Additional file 4: Figure S2 Distribution of SLAF tags in the barley genome

Additional file 5: Table S3 Screening of SNP markers

Additional file 6: Figure S3 Association analysis of cuticular wax-deficient gene using the SNP-index method

Declarations

Acknowledgments

We thank LetPub (www.letpub.com) for its linguistic assistance during the preparation of this manuscript.

Funding

This research was supported by the National Natural Science Foundation of China (31401316) and Hangzhou Scientific and Technological Program (20140432B03). The funding bodies had no role in the design of the study, the collection, analysis, and interpretation of data and in writing the manuscript.

Availability of data and materials

The data sets supporting the conclusions of this article are available by contacting with the corresponding author (dwxue@hznu.edu.cn). The varieties of barley collection are deposited in Hangzhou Normal University and provided on request in form of collaboration.

Authors' contributions

YF, XZ and DX designed the research, performed experiments, analyzed the data and wrote the manuscript. TT, ZZ, BT, JC, and JZ performed the research. All authors have read and approved the manuscript.

Ethics approval and consent to participate

Not applicable.

Consent for publication

Not applicable.

Competing interests

The authors declare that they have no competing interests.

References

1. Seo PJ, Park CM. Cuticular wax biosynthesis as a way of inducing drought resistance. Plant Signal Behav.2011; 6(7):1043-5.
2. Bernard A, Joubès J. Arabidopsis cuticular waxes: advances in synthesis, export and regulation. Progress in lipid research. 2013; 52(1), 110-29.
3. Yeats TH, Rose JK. The formation and function of plant cuticles. Plant Physiol. 2013; 163(1), 5-20.
4. Lee SB, Suh MC. Advances in the understanding of cuticular waxes in *Arabidopsis thaliana* and crop species. Plant Cell Rep. 2015; 34(4), 557-72.
5. Xue D, Zhang X, Lu X, Chen G, Chen ZH. Molecular and evolutionary mechanisms of cuticular wax for plant drought tolerance. Front Plant Sci. 2017; 8:
6. Weidenbach D, Jansen M, Franke RB, Hensel G, Weissgerber W, Ulferts S, Jansen I, Schreiber L, Korzun V, Pontzen R, et al. Evolutionary conserved function of barley and Arabidopsis 3-KETOACYL-CoA SYNTHASES in providing wax signals for germination of powdery mildew fungi. Plant Physiol. 2014; 166(3): 1621-33.
7. Wang W, Liu X, Gai X, Ren J, Liu X, Cai Y, Wang Q, Ren H. *Cucumis sativus* wax2 plays a pivotal role in wax biosynthesis, influencing pollen fertility and plant biotic and abiotic stress responses. Plant Cell Physiol. 2015; 56(7): 1339-54.
8. Hooker TS, Millar AA, Kunst L. Significance of the expression of the CER6 condensing enzyme for cuticular wax production in Arabidopsis. Plant Physiol. 2002; 129(4): 568-80.
9. Mao B, Cheng Z, Lei C, Xu F, Gao S, Ren Y, Wang J, Zhang X, Wang J, Wu F, et al. Wax crystal-sparse leaf2, a rice homologue of WAX2/GL1, is involved in synthesis of leaf cuticular wax. 2012; 235(1), 39-52.
10. Li C, Wang A, Ma X, Pourkheirandish M, Sakuma S, Wang N, Ning S, Nevo E, Nawrath C, Komatsuda T, Chen G. An eceriferum locus, *cer-zv*, is associated with a defect in cutin responsible for water retention in barley (*Hordeum vulgare*) leaves. Theor Appl Genet. 2013; 126(3): 637-46.
11. Li C, Ma X, Wang A, Nevo E, Chen G. Genetic mapping of cuticle-associated genes in barley. Cereal Res 2013; 41(1): 23-34.
12. Zhou Q, Li C, Mishina K, Zhao J, Zhang J, Duan R, Ma X, Wang A, Meng Q, Komatsuda T, Chen G. Characterization and genetic mapping of the β-diketone deficient *eceriferum-b barley* Theor Appl Genet. 2017; 130(6): 1169-78.
13. Chen, G., Sagi, M., Weining S, Krugman T, Fahima T, Korol AB, Nevo E. Wild barley *eibil* mutation identifies a gene essential for leaf water conservation. Planta. 2004; 219(4): 684-93.
14. Li C, Haslam T, Krüger A, Schneider LM, Mishina K, Samuels L, Yang H, Kunst L, Schaffrath U, Nawrath C, et al. The β-ketoacyl-CoA synthase *Hv*KCS1, encoded by *Cer-zh*, plays a key role in

synthesis of barley leaf wax and germination of barley powdery mildew. Plant Cell Physiol. 2018; 59(4): 806-22.

15. Hen-Avivi S, Savin O, Racovita RC, Lee WS, Adamski NM, Malitsky S, Almekias-Siegl E, Levy M, Vautrin S, Bergès H, et al. A metabolic gene cluster in the wheat *W1* and the barley *Cer-cqu* loci determines β-diketone synthesis and glaucousness. Plant Cell. 2016; 28(6): 1440-60.
16. Schneider LM, Adamski NM, Christensen CE, Stuart DB, Vautrin S, Hansson M, Uauy C, von Wettstein-Knowles P. The *Cer-cqu* gene cluster determines three key players in a β-diketone synthase polyketide pathway synthesizing aliphatics in epicuticular waxes. J Exp 2016; 67(9): 2715-30.
17. Mascher M, Gundlach H, Himmelbach A, Beier S, Twardziok SO, Wicker T, Radchuk V, Dockter C, Hedley PE, Russell J, et al. A chromosome conformation capture ordered sequence of the barley genome. Nature. 2017; 544(7651): 427-33.
18. Sun X, Liu D, Zhang X, Li W, Liu H, Hong W, Jiang C, Guan N, Ma C, Zeng H, et al. SLAF-seq: an efficient method of large-scale de novo SNP discovery and genotyping using high-throughput sequencing. PloS one. 2013; 8(3): e58700.
19. Zhang Y, Wang L, Xin H, Li D, Ma C, Ding X, Hong W, Zhang X. Construction of a high-density genetic map for sesame based on large scale marker development by specific length amplified fragment (SLAF) sequencing. BMC plant biol. 2013; 13(1): 141.
20. Li N, Yin Y, Wang F, Yao M. Construction of a high-density genetic map and identification of QTLs for cucumber mosaic virus resistance in pepper (*Capsicum annuum*) using specific length amplified fragment sequencing (SLAF-seq). Breeding science. 2018; 68(2): 233-41.
21. Zhang Y, Li W, Lin Y, Zhang L, Wang C, Xu R. Construction of a high-density genetic map and mapping of QTLs for soybean (*Glycine max*) agronomic and seed quality traits by specific length amplified fragment sequencing. BMC genomics. 2018; 19(1): 641.
22. Michelmore RW, Paran I, Kesseli RV. Identification of markers linked to disease-resistance genes by bulked segregant analysis: a rapid method to detect markers in specific genomic regions by using segregating populations. PNAS. 1991; 88(21): 9828-32.
23. Li Y, Zeng XF, Zhao YC, Li JR, Zhao DG. Identification of a new rice low-tiller mutant and association analyses based on the slaf-seq method. Plant molecular biology reporter. 2017; 35(1): 72-82.
24. Xu X, Lu L, Zhu B, Xu Q, Qi X, Chen X. QTL mapping of cucumber fruit flesh thickness by SLAF-seq. Scientific reports. 2015; 5: 15829.
25. Qin D, Dong J, Xu F, Guo G, Ge S, Xu Q, Xu Y, Li M. Characterization and fine mapping of a novel barley Stage Green-Revertible Albino Gene (*HvSGRA*) by Bulked Segregant Analysis based on SSR assay and Specific Length Amplified Fragment Sequencing. BMC Genomics. 2015; 16: 838.
26. Jia Q, Wang J, Zhu J, Hua W, Shang Y, Yang J, Liang Z. Toward identification of black lemma and pericarp gene Blp1 in barley combining bulked segregant analysis and specific-locus amplified fragment sequencing. Front Plant Sci. 2017; 8, 1414.
27. Hu MJ, Zhang HP, Liu K, Cao JJ, Wang SX, Jiang H, Wu ZY, Lu J, Zhu XF, Xia XC,et al. Cloning and Characterization of Gene Associated with Grain Weight in Wheat via SLAF-seq-BSA. Front Plant Sci.

2016; 7: 1902.

28. Zhao T, Jiang J, Liu G, He S, Zhang H, Chen X, Li J, Xu X. Mapping and candidate gene screening of tomato Cladosporium fulvum-resistant gene Cf-19, based on high-throughput sequencing technology. BMC Plant Biol. 2016; 16: 51.
29. Xu X, Chao J, Cheng X, Wang R, Sun B, Wang H, Luo S, Xu X, Wu T, Li Y. Mapping of a Novel Race Specific Resistance Gene to Phytophthora Root Rot of Pepper (*Capsicum annuum*) Using Bulked Segregant Analysis Combined with Specific Length Amplified Fragment Sequencing Strategy. PLoS ONE. 2016; 11: e0151401.
30. Abe A, Kosugi S, Yoshida K, Natsume S, Takagi H, Kanzaki H, Matsumura H, Yoshida K, Mitsuoka C, Tamiru M, Innan H, Cano L, Kamoun S, Terauchi R. Genome sequencing reveals agronomically important loci in rice using MutMap. Nat biotechnol. 2012; 30(2): 174.
31. Takagi H, Abe A, Yoshida K, Kosugi S, Natsume S, Mitsuoka C, Uemura A, Utsushi H, Tamiru M, Takuno S, Innan H, Cano LM, Kamoun S, Terauchi R. QTL-seq: rapid mapping of quantitative trait loci in rice by whole genome resequencing of DNA from two bulked populations. Plant J. 2013; 74(1): 174-83.
32. Neinhuis C, Barthlott W. Characterization and distribution of water-repellent, self-cleaning plant surfaces. Annals of botany. 1997; 79(6): 667-77.
33. Jeffree CE. The fine structure of the plant cuticle. Biology of the plant cuticle, 2006; 23: 11-125.
34. Koch K, Ensikat HJ. The hydrophobic coatings of plant surfaces: epicuticular wax crystals and their morphologies, crystallinity and molecular self-assembly. Micron. 2008; 39(7): 759-72.
35. Hen-Avivi S, Lashbrooke J, Costa F, Aharoni A. Scratching the surface: genetic regulation of cuticle assembly in fleshy fruit. J Exp Bot. 2014; 65(16): 4653-64.
36. Richardson A, Boscari A, Schreiber L, Kerstiens G, Jarvis M, Herzyk P, Fricke W. Cloning and expression analysis of candidate genes involved in wax deposition along the growing barley (Hordeum vulgare) leaf. Planta. 2007; 226(6): 1459-73.
37. Chen G, Komatsuda T, Ma JF, Nawrath C, Pourkheirandish M, Tagiri A, Hu YG, Sameri M, Li X, Zhao X, et al. An ATP-binding cassette subfamily G full transporter is essential for the retention of leaf water in both wild barley and rice. PNAS. 2011; 108(30): 12354-9.
38. Richardson A, Franke R, Kerstiens G, Jarvis M, Schreiber L, Fricke W. Cuticular wax deposition in growing barley (Hordeum vulgare) leaves commences in relation to the point of emergence of epidermal cells from the sheaths of older leaves. Planta. 2005; 222(3): 472-83.
39. Pollard M, Beisson F, Li Y, Ohlrogge JB. Building lipid barriers: biosynthesis of cutin and suberin. Trends Plant Sci. 2008; 13(5):236-46.
40. Fich EA, Segerson NA, Rose JK. The plant polyester cutin: biosynthesis, structure, and biological roles. Annu Rev Plant Biol. 2016; 67, 207-33.
41. Zhang XF, Wang GY, Dong TT, Chen B, Du HS, Li CB, Zhang FL, Zhang HY, Xu Y, Wang Q, Geng SS. High-density genetic map construction and QTL mapping of first flower node in pepper (*Capsicum annuum*). BMC plant biol. 2019; 19(1): 167.

42. Lu Z, Niu L, Chagné D, Cui G, Pan L, Foster T, Zhang R, Zeng W, Wang Z. Fine mapping of the temperature-sensitive semi-dwarf (Tssd) locus regulating the internode length in peach (*Prunus persica*). breeding. 2016; 36(2), 20.
43. Zhang XQ, Xue DW, Zhou WH, Wu FB, Zhang GP. Screening and identification of the mutants from two-row barley cultivar ZJU3 induced by ethyl methane sulfonate (EMS). J Zhejiang Univ (Agric. & Life Sci.). 2011; 37(2): 169-74.

Figures

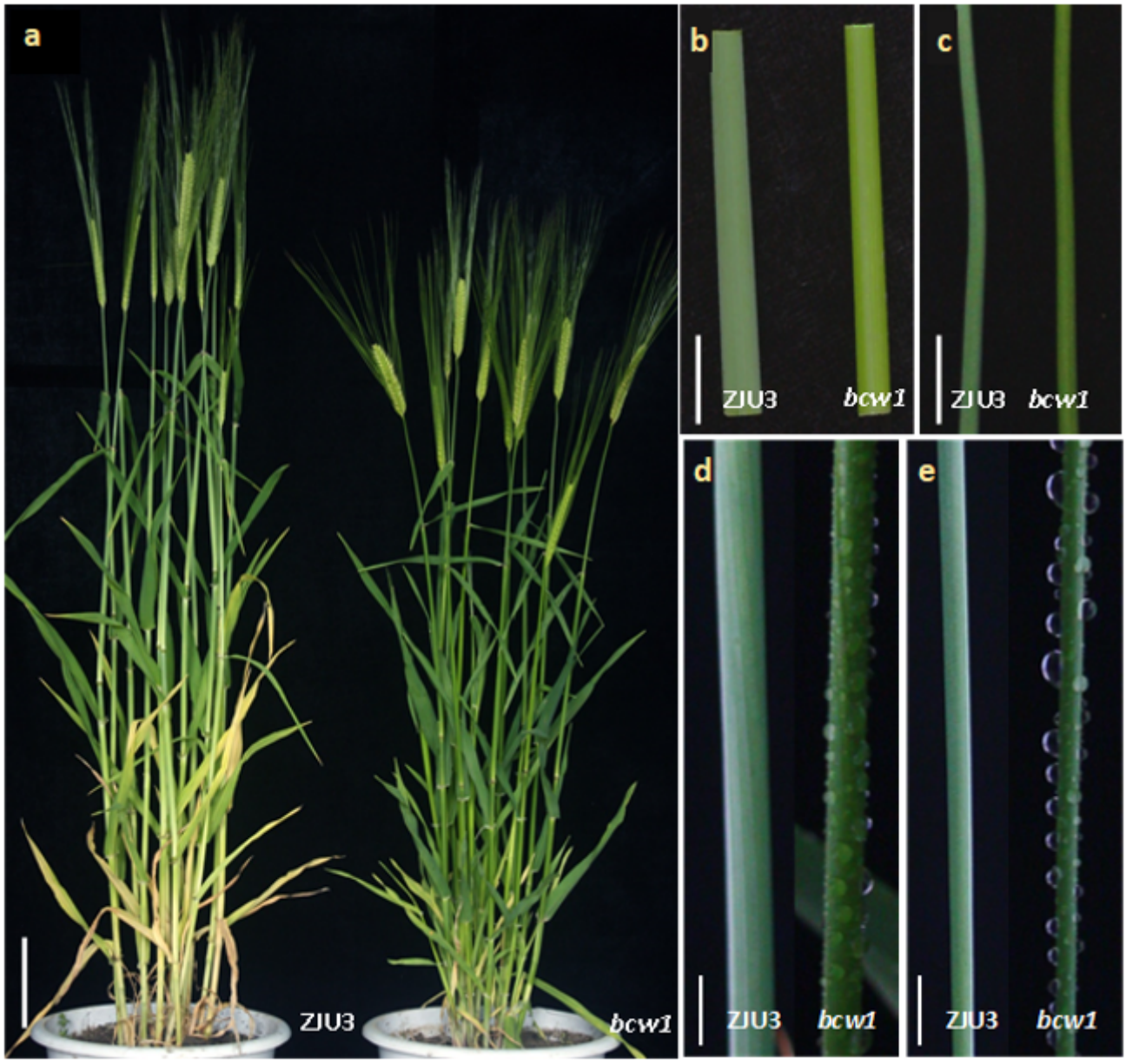

Figure 1

The phenotypes of wild type (ZJU3) and bcw1. The whole plants and different tissues of wild type and mutant were observed, and water droplet arrays were carried out to confirm the observations. a Plants at grain filling stage. Scale bars =10cm. b and c Blade sheaths and stems. Scale bars = 2cm and 1cm. d and e Water droplets on the surface of the sheaths and stems. Scale bars =1cm

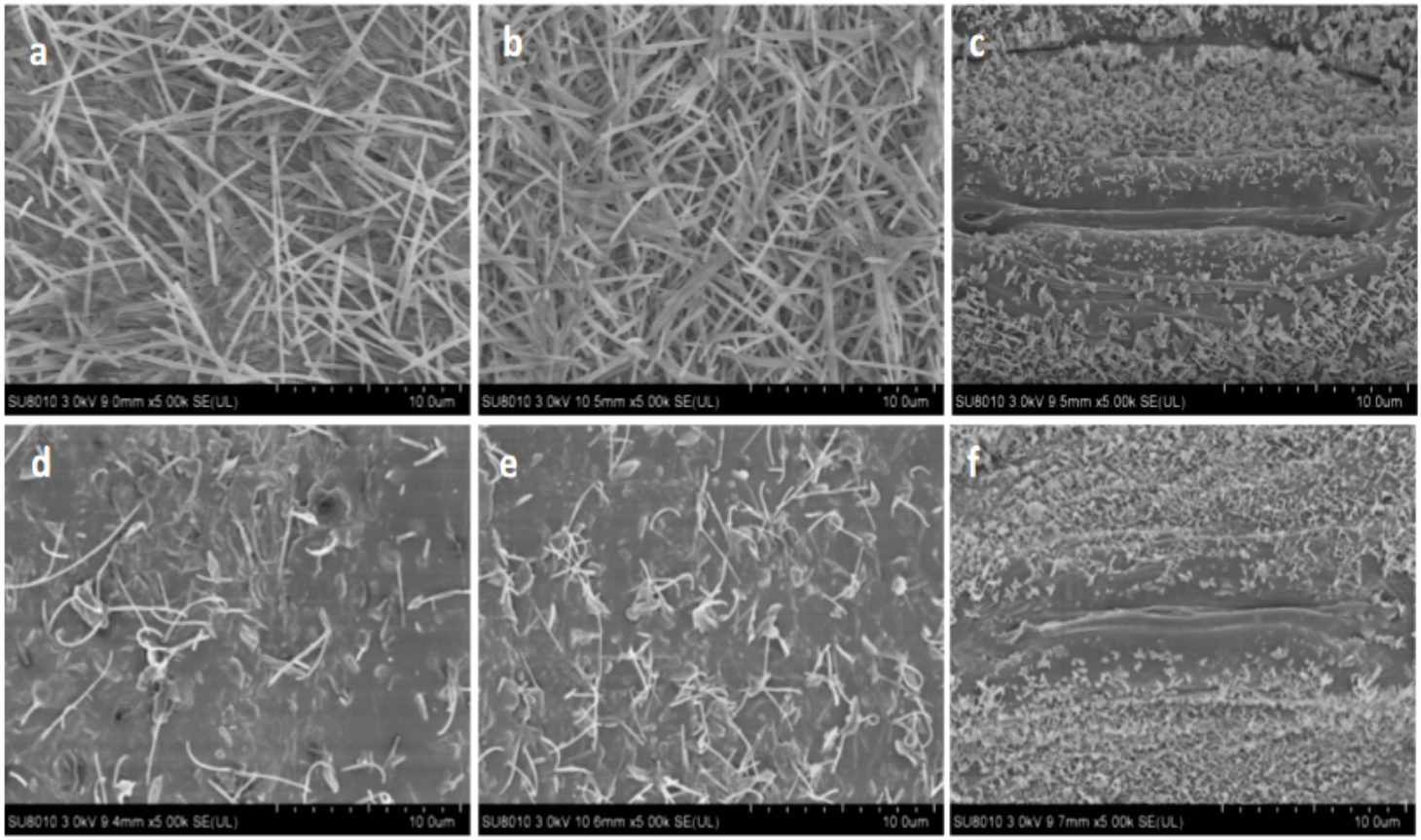

Figure 2

Epicuticular wax crystals on stem, sheath and leaf surfaces of bcw1 and ZJU3. Platelet-shaped crystals distributing on leaf surfaces and tubule-shaped crystals distributing on stem and sheath surfaces of bcw1 and ZJU3 were observed by SEM. a, b, c Crystals on stem, sheath and leaf surfaces of mutant. d, e, f Crystals on stem, sheath and leaf surfaces of wild type. Scale bars=10μm.

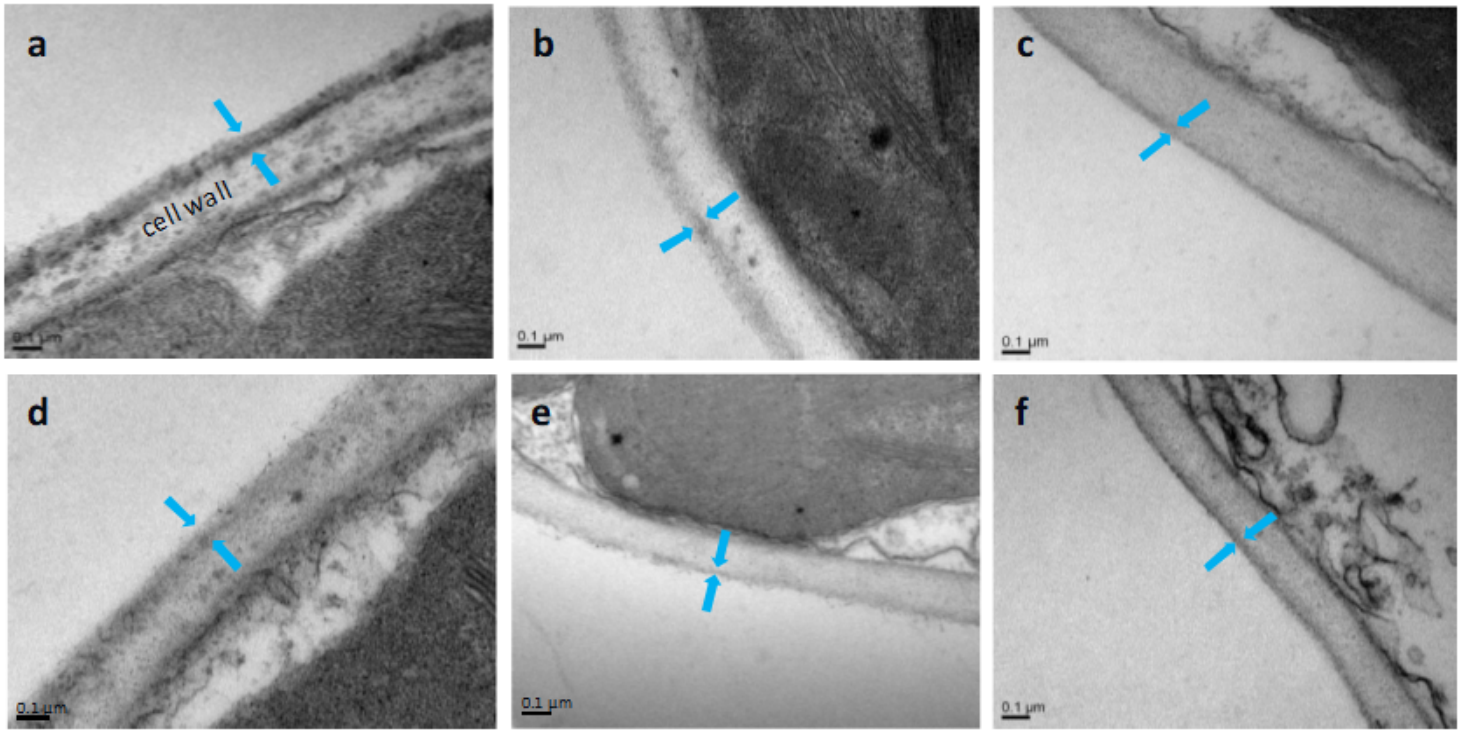

Figure 3

Cuticles of wild type and mutant leaves, sheaths and stems. Cuticles outside the epidermal cells of wild type and mutant leaves, sheaths and stems were observed by TEM, and abberant cuticles were formed on the mutant stems and sheaths. a, b, c Stem, sheath and leaf cuticles of wild type. d, e, f Stem, sheath and leaf cuticles of bcw1. Scale bar=0.1μm.

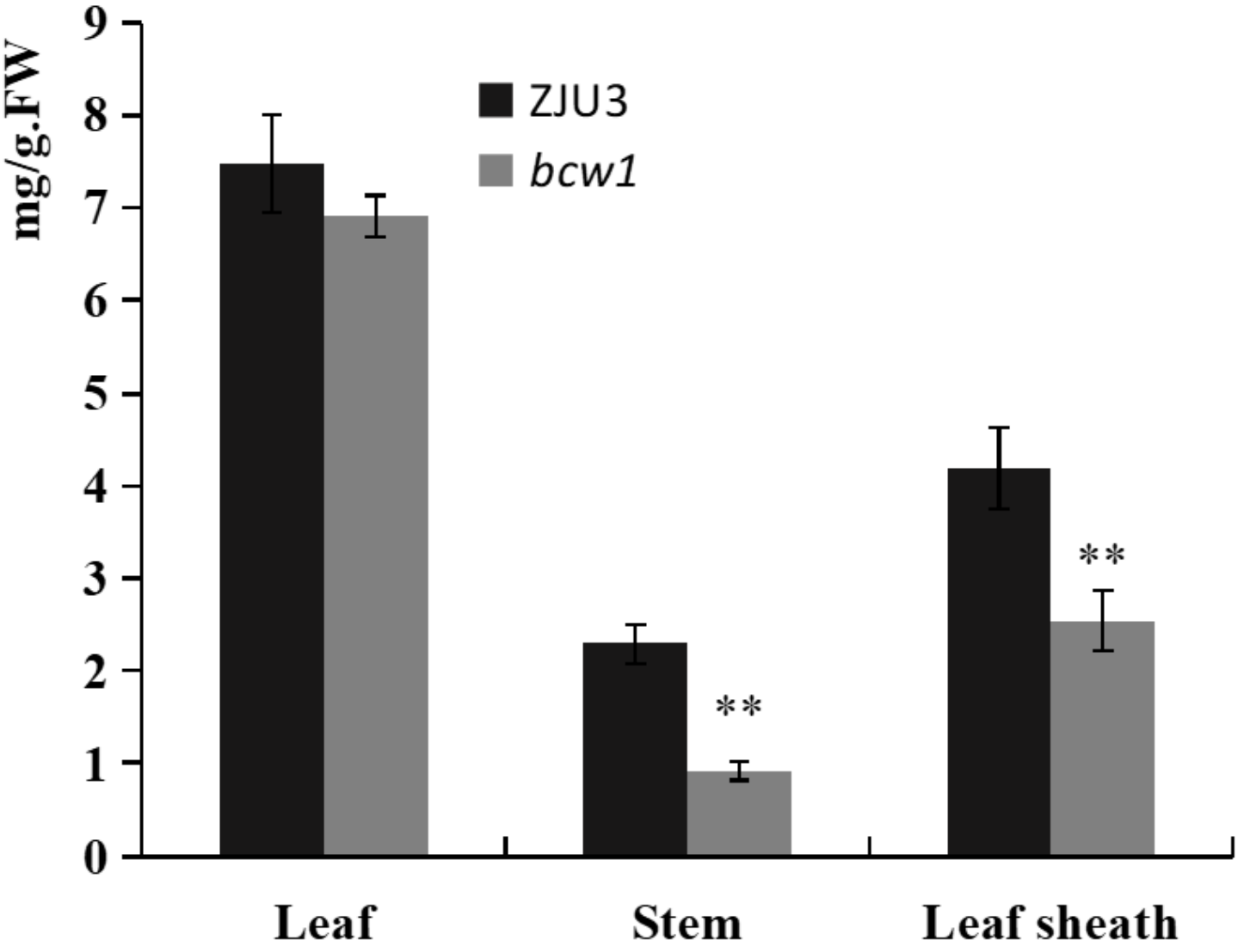

Figure 4

The total wax extracted from leaves, stems and leaf sheaths of bcw1 and ZJU3. The x-axis indicates the different tissues of bcw1 and ZJU3, and the y-axis represents the total cuticular wax contents per gram fresh weight (mg/g.FW). ** indicates highly significant (P<0.01).

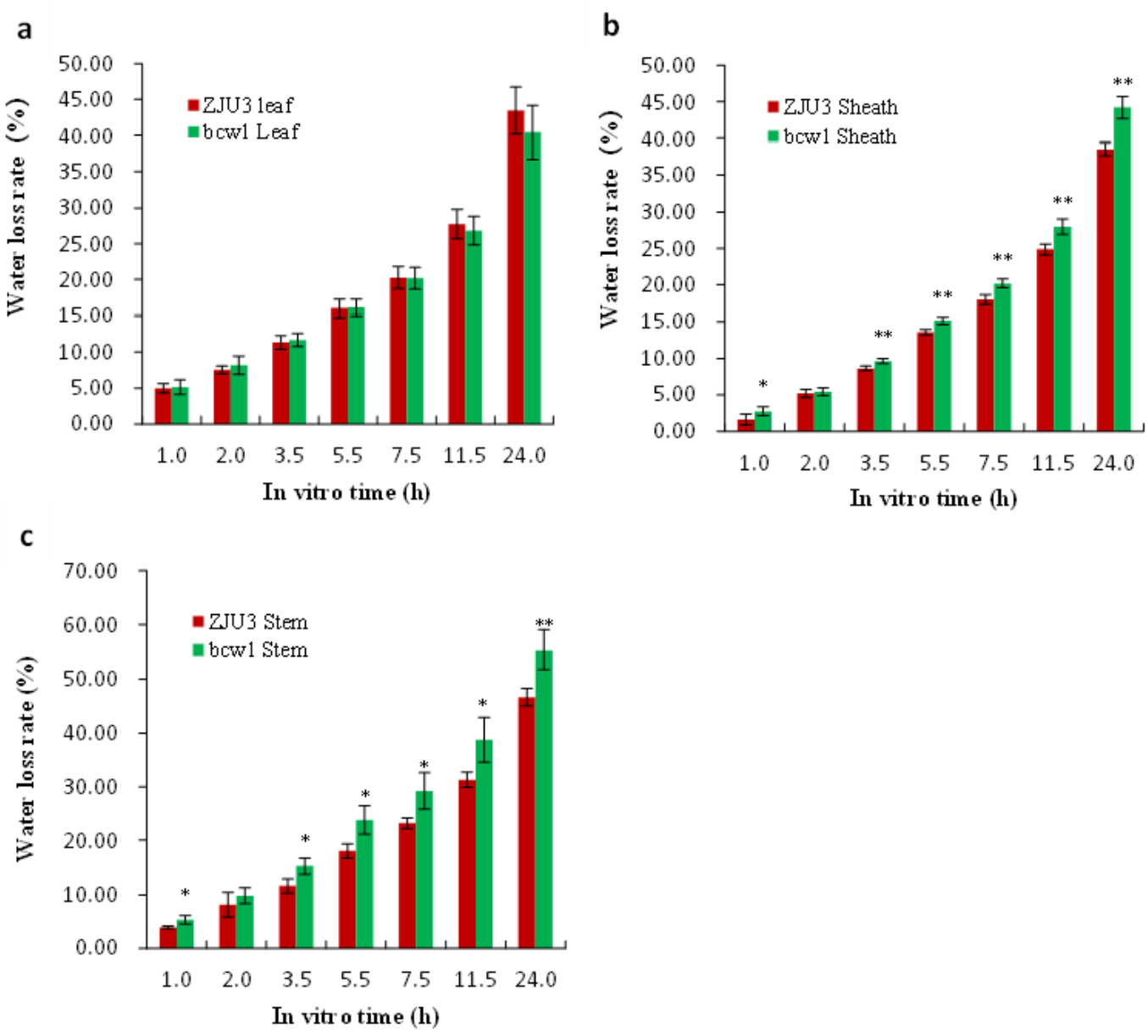

Figure 5

Water loss rate of detached leaves, stems and leaf sheaths of ZJU3 and bcw1. The x-axis and y-axis represent the in vitro time (h) and water loss rate of detached tissues, respectively. a, b, c Water loss of bcw1 and ZJU3 leaves, sheaths and stems. * indicates significant ($P<0.05$), and ** indicates highly significant ($P<0.01$).

Supplementary Files

This is a list of supplementary files associated with this preprint. Click to download.

- AdditionalfilesBCW1.docx